The Oncologist®

Gastrointestinal Cancer

Mismatch Repair Status of Gastric Cancer and Its Association with the Local and Systemic Immune Response

Su-Jin Shin,[a] Sang Yong Kim,[b] Yoon Young Choi,[c] Taeil Son,[c] Jae-Ho Cheong,[c] Woo Jin Hyung,[c,d] Sung Hoon Noh,[c] Chung-Gyu Park,[e,f] Hyoung-Il Kim[b,c,d,e,f]

[a]Department of Pathology, College of Medicine, Hanyang University, Seoul, Republic of Korea; [b]Open NBI Convergence Technology Research Laboratory, Severance Hospital, Yonsei University Health System, Seoul, Republic of Korea; [c]Department of Surgery, Yonsei University College of Medicine, Seoul, Republic of Korea; [d]Robot and Minimally Invasive Surgery Center, Yonsei University Health System, Seoul, Republic of Korea; [e]Translational Xenotransplantation Research Center and [f]Department of Microbiology and Immunology, Seoul National University College of Medicine, Seoul, Republic of Korea

Disclosures of potential conflicts of interest may be found at the end of this article.

Key Words. Gastric cancer • Microsatellite instability • Tumor-infiltrating lymphocytes • Survival

Abstract

Background. Microsatellite instability (MSI)-high (MSI-H) colorectal cancer is known to be associated with increased tumor-infiltrating lymphocytes (TILs), elevated host systemic immune response, and a favorable prognosis. In gastric cancer, however, MSI status has rarely been evaluated in the context of TILs and systemic immune response.

Materials and Methods. We evaluated data for 345 patients with gastric cancer who underwent gastrectomy with MSI typing. The numbers of TILs were counted after immunohistochemical staining with anti-CD3, CD4, CD8, forkhead box P3 (Foxp3), and granzyme B to quantify the subsets of TILs. To evaluate the systemic immune response, the differential white blood cell count and prognostic nutritional index (PNI) were obtained.

Results. Of the 345 patients, 57 demonstrated MSI-H tumors and 288 demonstrated non-MSI-H tumors. MSI-H tumors carried significantly higher densities of CD8+ T cells, Foxp3+ T cells, and granzyme B+ T cells and a higher ratio of Foxp3/CD4 and granzyme B/CD8. The prognostic impact of TILs differed between patients with MSI-H tumors and those with non-MSI-H tumors. The TIL subsets were not found to be significant prognostic factors for recurrence-free survival (RFS) or overall survival (OS) in the MSI-H tumor group. In the non-MSI-H tumor group, multivariate analysis showed that stage, PNI, and CD4+ T cells were independent prognostic factors for RFS, and stage, PNI, and the Foxp3/CD4 ratio were independent prognostic factors for OS.

Conclusions. The association between systemic/local immune response and prognosis differed according to MSI status. Different tumor characteristics and prognoses according to MSI status could be associated with the immunogenicity caused by microsatellite instability and subsequent host immune response. ***The Oncologist*** 2019;24:e835–e844

Implications for Practice: This study demonstrates that the density of each subset of tumor-infiltrating lymphocytes (TILs) differed between microsatellite instability (MSI)-high and non-MSI-high tumors. Moreover, the prognostic effect of the preoperative systemic immune response status and TILs differed between the MSI-high (MSI-H) and non-MSI-H tumor groups. The present study may help to identify the mechanisms of cancer progression and develop treatment strategies for MSI-high gastric cancer.

Introduction

The immune microenvironment of a tumor has been recognized as an important determinant of the biological and clinical characteristics of cancer [1]. Although previous studies have focused on only the oncological characteristics of cancer, the relationship between cancer and the host immune system has gained more interest [2, 3].

Microsatellite instability (MSI)-high (MSI-H) tumors are caused by defective DNA mismatch repair systems and are known to have higher levels of tumor-infiltrating lymphocytes (TILs) and favorable prognoses [4–6]. One explanation for this characteristic is that frameshift-mutated peptides generated by MSI may be easily recognized by the host immune system and can induce an immune response [7, 8]. The frame-shift mutation and generation of immunogenic peptides are proposed mechanisms of increased TILs and favorable prognoses in MSI-H type colon cancer [9, 10]. The

Correspondence: Hyoung-Il Kim, M.D., Department of Surgery, Yonsei University College of Medicine, 50-1, Yonsei-ro, Seodaemun-gu, Seoul 03722, Republic of Korea. Telephone: 82-2-2228-2100; e-mail: cairus@yuhs.ac Received May 8, 2018; accepted for publication February 13, 2019; published Online First on March 20, 2019. http://dx.doi.org/10.1634/theoncologist.2018-0273

relationship between TILs and MSI in colon cancer has been studied extensively; however, much remains to be studied in terms of gastric cancer.

MSI-H gastric cancer accounts for approximately 10% of MSI-H tumors, and studies have shown that patients with MSI-H gastric cancer have better prognoses and higher levels of TILs than those with non-MSI-H gastric cancer [11–13]. Although TILs are considered prognostic factors in gastric cancer as well as in other human malignancies [2, 14–17], TILs in association with genetic alterations are rarely studied in gastric cancer [4, 18]. Given the prognostic and predictive relevance of TILs and MSI phenotype, a clear understanding of the link between the host immune response and genetic alterations is crucial.

The systemic inflammatory response status is thought to be secondary to hypoxia or tumor necrosis. Many studies have shown that the preoperative serum systemic inflammatory response, including the serum albumin level, C-reactive protein (CRP), absolute neutrophil count (ANC), absolute lymphocyte count (ALC), and a combination of such factors including the neutrophil/lymphocyte ratio (NLR), platelet-to-lymphocyte ratio (PLR), and the prognostic nutritional index (PNI) have prognostic values in many cancer and hematologic malignancies [19–21]. However, the value of the systemic inflammatory response status has rarely been studied within the context of TILs, and it is unclear whether the systemic inflammatory response is associated with TILs or not [22, 23]. Wang et al. showed that PLR and TILs are independent prognostic factors in patients with laryngeal squamous cell carcinoma [24]. Turner et al. combined the results of TILs and NLR and showed that low TILs and high NLR is associated with poor outcome in stage II colon cancer, and no significant relationship was identified between local and systemic inflammation [25]. Park et al. revealed the relationships with CD3+ T cells and elevated systemic immune response, such as circulating CRP, ANC, and platelet counts in MSI-H colorectal cancer [23]. In a recent gastric cancer study, the author showed that a high density of CD4+ T cells in tumor stroma is associated with low NLR and high PNI. However, the authors did not show MSI status [26].

Therefore, we examined the MSI status of gastric cancer and its association with the local immune response (subsets of TILs) and systemic immune response (ANC, ALC, NLR, and PNI) to evaluate the prognostic significance.

Materials and Methods

Patients

We retrospectively analyzed a database of patients with gastric cancer who underwent gastrectomy at Severance Hospital, Yonsei University College of Medicine, from January 1996 to December 2011. Inclusion criteria were pathologically proven gastric adenocarcinoma treated via curative surgical resection and available data regarding MSI typing. Patients with a family history of hereditary nonpolyposis colorectal cancer or Lynch syndrome, distant metastasis at the time of diagnosis, a history of neoadjuvant chemotherapy or radiation therapy, a history of other primary cancers, and Epstein-Barr virus-positive gastric carcinoma, as well as those who died within 30 days of surgery, were excluded. Finally, 345 patients, 57 with MSI-H and 288 with non-MSI-H gastric cancers (278 microsatellite stable and 10 low microsatellite instable), were selected. The staging was conducted according to the American Joint Committee on Cancer, 7th Edition [27].

The preoperative ANC and ALC were obtained from the routine complete blood count with four-part differential (lymphocytes, monocytes, eosinophils, and neutrophils) counts. The PNI was calculated by using the following equation [28]: (10 × serum albumin [g/dL]) + (0.005 × total lymphocyte count). All laboratory data were obtained at the time of the diagnosis. The study protocol conformed to the ethical guidelines of the 1975 Declaration of Helsinki and was approved by the Yonsei Institutional Review Board (4-2010-0023).

Microsatellite Analysis

DNA extraction and microsatellite analysis were performed as previously described [29]. In brief, DNA was extracted from formalin-fixed, paraffin-embedded tissues using the QIAamp DNA mini kit (Qiagen, Hilden, Germany). The microsatellite analysis was performed using a panel of five National Cancer Institute workshop-recommended consensus microsatellite markers (BAT25, BAT26, D2S123, D17S250, and D5S346) [30]. Polymerase chain reaction (PCR) was performed using a fluorescence-labeled multiprimer, HotStarTaq polymerase (Qiagen) and the GeneAmp PCR system 2700 (Applied Biosystems, Foster City, CA). Amplifications were performed with an initial denaturation step at 95°C for 15 min, followed by 30 cycles of 1 min each at 95°C, 1 min at 57°C, and 1 min at 72°C. The amplification was completed with a final 5 min at 72°C. The amplified PCR products were analyzed using the automated ABI PRISM sequencer model 3100 genetic analyzer (Applied Biosystems). Cases showing the shifting of microsatellites at two or more markers were classified as MSI-H. Cases showing MSI at less than two markers were classified as non-MSI-H.

Immunohistochemical Staining and Interpretation of Mismatch Repair Protein

Immunohistochemical stains were performed using the Ventana Benchmark XT automated staining system (Ventana Medical Systems, Tucson, AZ) according to the manufacturer's protocol. The following primary antibodies were used for immunohistochemistry: MLH1 (G168–728; Cell Marque, Rocklin, CA), PMS2 (1:40; MRQ-28; Cell Marque), MSH2 (G219-1129; Cell Marque), and MSH6 (1:100; 44; Cell Marque). Loss of staining was defined as complete loss of nuclear staining in all of the tumor nuclei with preserved staining of lymphocytes and/or nonneoplastic gastric foveolar epithelium.

Immunohistochemical Staining of TILs

Immunohistochemical staining was performed as previously described [31]. Archival formalin-fixed, paraffin-embedded tissue obtained at initial diagnosis was available for all patients, and for each case, a block was chosen that contained a representative lesion of invasive tumor. Each block was serially sectioned for hematoxylin-eosin staining and five immunohistochemical staining. The sections were deparaffinized in xylene and rehydrated in decreasing concentrations of ethanol. Antigen retrieval was performed in citrate buffer in a microwave. Endogenous peroxidase activity was blocked by incubating the samples in 3% hydrogen peroxide in methanol for 5 min. The sections were incubated for 60 min at room temperature with the following

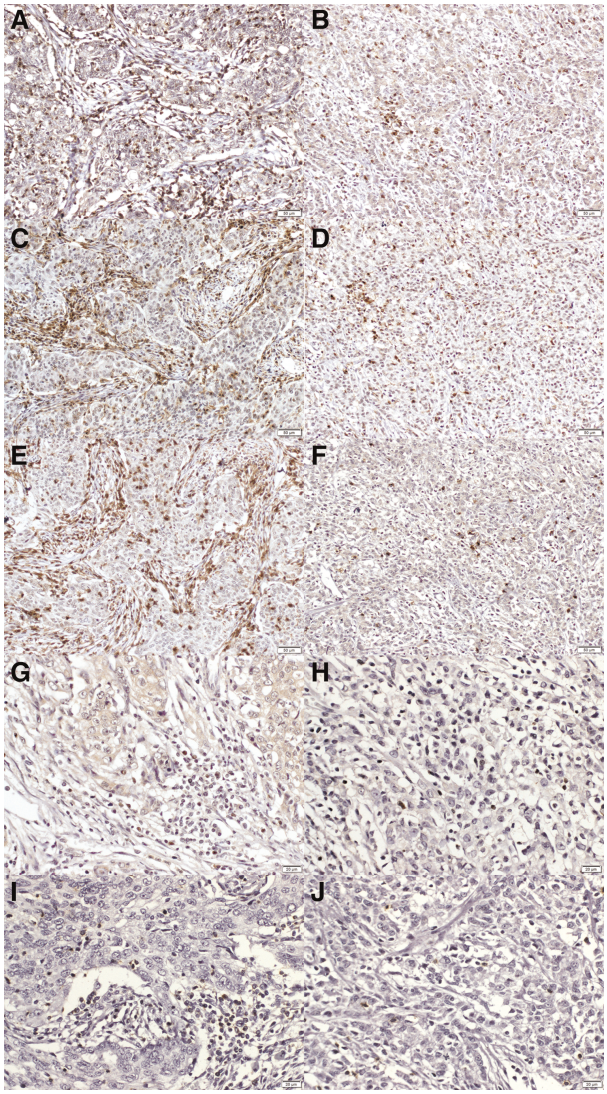

Figure 1. Immunohistochemical staining of tumor-infiltrating lymphocytes according to microsatellite instability (MSI) status. MSI-high (MSI-H) and non-MSI-H tumors are shown stained with **(A, B)** CD3 for total T lymphocytes; **(C, D)** CD4 for helper T lymphocytes; **(E, F)** CD8 for cytotoxic T lymphocytes; **(G, H)** forkhead box P3 for regulatory T lymphocytes; and **(I, J)** granzyme B for activated cytotoxic T lymphocytes [**(A–F)** × 200; **(G–J)** × 400].

primary monoclonal antibodies: CD3 (Fig. 1A, 1B; 1:100; LabVision Corporation, Fremont, CA), CD4 (Fig. 1C, 1D; 1:100; Novocastra, Newcastle upon Tyne, U.K.), CD8 (Fig. 1E, 1F; 1:100; Novocastra), forkhead box P3 (Foxp3; Fig. 1G, 1H; 1:100; ab20034; Abcam, Cambridge, U.K.), and granzyme B (GZB; Fig. 1I, 1J; 1:100; LabVision Corporation). They were used to identify the following T lymphocyte subsets: total T lymphocytes, helper T lymphocytes, cytotoxic T lymphocytes, regulatory T cells, and activated cytotoxic T lymphocytes, respectively. Incubation with horseradish peroxidase-conjugated secondary antibodies was subsequently performed, followed by development with diaminobenzidine and counterstaining with hematoxylin. Between solution changes, the slides were rinsed twice in 0.05 mol/L Tris-buffered saline with 0.2% Tween-20. Normal human tonsil was used as positive control. The negative control for immunostaining was prepared by incubating tissue sections without the primary antibody.

Quantification of TILs

An experienced pathologist (S.J.S.) who was blinded to the patient data reviewed the H&E slide of each case. The analysis was performed in the tumor center, as well as the center of four tumor quadrants within the borders of invasive cancer. A representative high-power field (×400) was chosen for each area and captured as an image. Areas of the tumor with necrosis or hemorrhage and areas of the stroma with a few tumor glands (less than 10% of total area) were avoided. The number of cells with positive reactions to each antibody was counted using the Image J software package (http://rsb.info.nih.gov/ij). The mean numbers of positively stained cells in each area were recorded. Subsequently, the absolute number of positive cells per high-power field (×400) was calculated (the mean number of positive cells in the five areas was added and divided by 5) for each antibody (CD3, CD4, CD8, Foxp3, and GZB). The ratios of Foxp3/CD4 and GZB/CD8 were also calculated.

Statistical Analysis

The clinical variables evaluated were age, sex, Lauren classification, histologic grade, depth of invasion, nodal status, and stage. Categorical data were compared using Pearson's chi-square, and the Mann-Whitney *U* test was used to evaluate associations with continuous variables. To estimate the overall survival (OS), patients were followed up from the date of surgical excision of the primary gastric tumor until the date of death. Likewise, to estimate the recurrence-free survival (RFS), patients were followed up from the date of surgical excision of the primary gastric tumor until the date of the first recurrence. Survival curves were constructed using the Kaplan-Meier method, the median count number was used to divide the patients into low- and high-density groups, and the log-rank test was used to evaluate the statistical significance. Cox proportional hazard models were used to conduct the univariate and multivariate analyses. A statistical significance level was defined as a p value <.05. All statistical analyses were performed using the SPSS statistical software version 21 (SPSS Inc., Chicago, IL).

Results

Patient Characteristics

The median follow-up period for the patients in this study was 88 months (range, 2–225 months). Of the total 345 patients, 153 (44.3%) died by the time of the analysis, and the median survival duration between the date of surgical excision and the date of death was 131 months. The estimated 5-year OS and RFS rates were 65.7% and 65.9%, respectively. Among 57 MSI-H gastric cancers, 35 were evaluated with immunohistochemistry for MLH1, PMS2, MSH2, and MSH6. Of these, 13 showed combined loss of MLH1 and PMS2 (13/35, 37.1%), 1 showed combined loss of MSH2 and MSH6 (1/35, 2.9%), 16 showed isolated loss of PMS2 (16/35, 45.7%) and 5 showed isolated loss of MSH6 (5/35, 14.3%).

Clinicopathologic Features and the Systemic and Local Immune Response According to MSI Status

Patients with MSI-H tumors were significantly older than those with non-MSI-H tumors (Table 1; 62.2 ± 13.7 and

Table 1. Clinicopathologic and tumor-infiltrating lymphocytic characteristics according to MSI status in patients with gastric carcinoma (n = 345)

	MSI phenotype		
Variables	**MSI-H (n = 57)**	**Non-MSI-H[a] (n = 288)**	**p value**
Mean age ± SD, yr	62.2 ± 13.7	57.7 ± 13.4	.020[b]
Sex, n (%)			.916[c]
Male	36 (63.2)	184 (63.9)	
Female	21 (36.8)	104 (36.1)	
Mean BMI ± SD, kg/m^2	23.2 ± 3.1	23.1 ± 3.2	.575[b]
Histology,[d] n (%)			.103[c]
Differentiated	29 (50.9)	113 (39.2)	
Undifferentiated	28 (49.1)	175 (60.8)	
Lauren classification, n (%)			.052[c]
Intestinal	36 (63.2)	141 (49.0)	
Diffuse	11 (19.3)	103 (35.8)	
Mixed	10 (17.5)	44 (15.3)	
Mean tumor size[e] ± SD, mm	56.6 ± 30.6	49.3 ± 29.9	.064[b]
pT category, n (%)			
pT1	11 (19.3)	59 (20.5)	.576[c]
pT2	8 (14.0)	47 (16.3)	
pT3	18 (31.6)	66 (22.9)	
pT4	20 (35.1)	116 (40.3)	
Nodal status, n (%)			.045[c]
Negative	33 (57.9)	125 (43.4)	
Positive	24 (42.1)	163 (56.6)	
Stage,[f] n (%)			.132[c]
I	17 (29.8)	80 (27.8)	
II	22 (38.6)	79 (27.4)	
III	18 (31.6)	129 (44.8)	
Lymphatic invasion, n (%)			.468[c]
Negative	12 (36.4)	93 (43.1)	
Positive	21 (63.6)	123 (56.9)	
Vascular invasion, n (%)			.969[c]
Negative	18 (45.0)	109 (44.7)	
Positive	22 (55.0)	135 (55.3)	
Neural invasion, n (%)			.839[c]
Negative	18 (56.3)	113 (54.3)	
Positive	14 (43.8)	95 (45.7)	
Mean ANC ± SD, cells/μL	4,184.3 ± 1,641.0	4,238.1 ± 1970.3	.987[b]
Mean ALC ± SD, cells/μL	2,089.5 ± 606.2	2039.6 ± 636.4	.524[b]
Mean NLR ± SD, ANC/ALC	2.2 ± 1.0	2.3 ± 1.4	.920[b]
Mean PNI ± SD	51.2 ± 6.4	52.9 ± 5.9	.154[b]
Mean CD3+ T cells ± SD	187.2 ± 67.4	169.8 ± 57.5	.056[b]
Mean CD4+ T cells ± SD	106.0 ± 53.9	99.1 ± 49.3	.329[b]
Mean CD8+ T cells ± SD	100.9 ± 44.0	77.2 ± 34.5	<.001[b]
Mean Foxp3+ T cells ± SD	28.0 ± 13.9	19.0 ± 14.3	<.001[b]
Mean GZB+ T cells ± SD	28.2 ± 19.4	19.0 ± 15.3	<.001[b]
Mean Foxp3/CD4 ± SD	34.7 ± 23.5	22.7 ± 21.5	<.001[b]
Mean GZB/CD8 ± SD	30.5 ± 20.7	27.9 ± 26.3	.036[b]

[a]Non-MSI-H: microsatellite stable (MSS) and MSI-low.
[b]Mann-Whitney U test.
[c]Two-sided Pearson's chi-square test.
[d]Differentiated: well-differentiated, moderately differentiated adenocarcinoma; undifferentiated: poorly differentiated, mucinous, signet ring cell carcinoma.
[e]Tumor size: greatest dimension.
[f]AJCC 7th edition.
Abbreviations: ALC, absolute lymphocyte count; ANC, absolute neutrophil count; BMI, body mass index; Foxp3, forkhead box P3; GZB, granzyme B; MSI, microsatellite instability; MSI-H, MSI-high; NLR, neutrophil lymphocyte ratio; PNI, prognostic nutritional index; pT, pathologic T category.

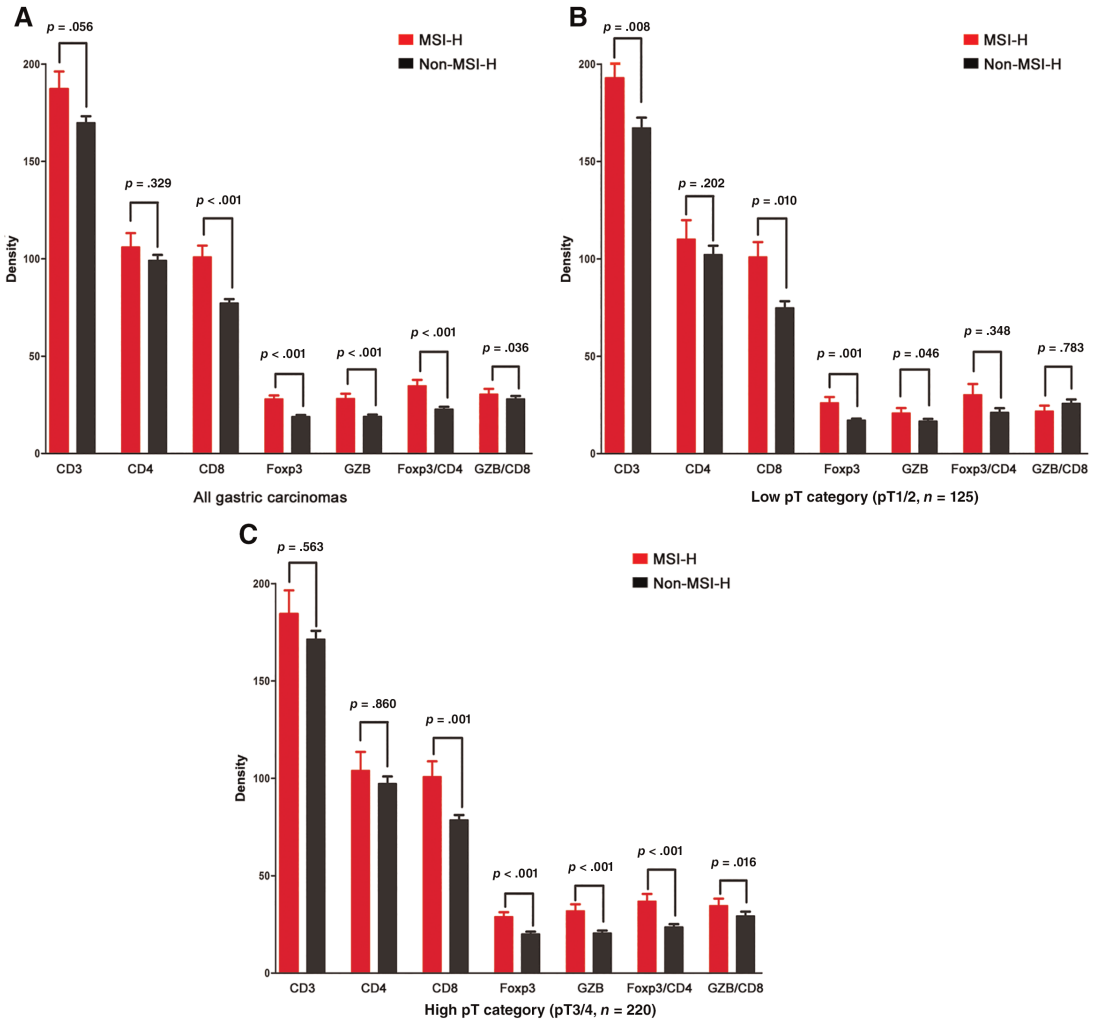

Figure 2. Density for each subset of tumor-infiltrating lymphocytes according to microsatellite instability (MSI) status. The gastric carcinomas with the MSI-H phenotype had a significantly higher number of CD8-, Foxp3-, and GZB-positive lymphocytes and a higher ratio of Foxp3/CD4 and GZB/CD8 **(A)**. These characteristic differences increased from the low pT group **(B)** to the high pT group **(C)**. Abbreviations: GZB, granzyme B; Foxp3, forkhead box P3; MSI-H, MSI-high; pT, pathologic T category.

57.7 ± 13.4 years, respectively; p = .020). Moreover, lymph node metastasis was more frequently observed in the non-MSI-H tumor group (p = .045). There were no associations between MSI status and other clinicopathologic features. Additionally, no correlation between the systemic inflammatory response (ANC, ALC, NLR, and PNI) and MSI status was identified.

Both the MSI-H and non-MSI-H tumor groups showed relatively similar densities (absolute number of positive cells per high-power field) of total infiltrated T lymphocytes (Fig. 2A; CD3; p = .056) and helper T lymphocytes (CD4; p = .329). The MSI-H tumor group showed significantly increased densities of cytotoxic T lymphocytes (CD8; p < .001), activated cytotoxic T lymphocytes (GZB; p < .001), and regulatory T lymphocytes (Foxp3; p < .001) when compared with the non-MSI-H tumor group. The ratios of Foxp3/CD4 and GZB/CD8 were also significantly higher in the MSI-H tumor group (p < .001 and p = .036, respectively).

In subgroup analysis according to pathological T (pT) classification, this characteristic difference was more prominent in the high pT subgroup (pT3/4) than in the low pT subgroup (pT1/2; Fig. 2B, 2C).

Association Between the Local and Systemic Immune Response

Local immune responses (TILs) showed a poor correlation with systemic immune responses (ANC, ALC, NLR, and PNI), with only a marginal negative association between PNI and GZB (p = .036; supplemental online Fig. 1).

Survival Analysis

We observed a significant difference in survival according to disease stage (all p < .001; supplemental online Fig. 2A, 2B), whereas MSI status did not appear to significantly affect RFS or OS (p = .072 and p = .159; supplemental Fig. 2C, 2D). However, patients with MSI-H tumors tended to demonstrate better RFS and OS than those with non-MSI-H tumors. The estimated 5-year RFS of patients with MSI-H tumors and those with non-MSI-H tumors was 77.9% and 63.6%, respectively; the estimated 5-year OS was 73.6% and 64.1%, respectively.

The univariate survival analysis for recurrence after surgical resection showed that age, sex, Lauren classification, tumor size, stage, lymphatic invasion, vascular invasion, neural invasion, ALC, PNI, CD3, and CD4 were significantly

Table 2. Univariate and multivariate Cox regression analyses for overall survival and recurrence-free survival according to clinicopathologic variables, MSI status, and subset of tumor-infiltrating lymphocytes in patients with gastric carcinoma (n = 345)

	Recurrence-free survival		Overall survival	
Variables	**HR (95% CI)**	***p* value**	**HR (95% CI)**	***p* value**
Univariate analysis				
Age[a]	0.977 (0.965–0.989)	<.001	1.001 (0.989–1.013)	.886
Sex (Female vs. male)	1.460 (1.022–2.088)	.038	1.017 (0.732–1.415)	.918
BMI[a]	0.950 (0.896–1.008)	.091	0.951 (0.903–1.002)	.062
Lauren classification (diffuse vs. intestinal, mixed)	1.583 (1.104–2.270)	.012	1.132 (0.810–1.583)	.468
Tumor size[a]	1.011 (1.008–1.015)	<.001	1.010 (1.006–1.014)	<.001
Stage[b]	3.586 (2.649–4.856)	<.001	2.131 (1.705–2.664)	<.001
Lymphatic invasion (positive vs. negative)	3.661 (2.177–6.156)	<.001	2.126 (1.395–3.241)	<.001
Vascular invasion (positive vs. negative)	3.662 (2.295–5.8420)	<.001	2.442 (1.650–3.615)	<.001
Neural invasion (positive vs. negative)	2.927 (1.854–4.620)	<.001	1.912 (1.281–2.854)	.002
MSI phenotype (non-MSI-H vs. MSI-H)	0.605 (0.347–1.055)	.077	0.718 (0.452–1.142)	.162
ANC[a]	1.000 (1.000–1.000)	.482	1.000 (1.000–1.000)	.175
ALC[a]	0.999 (0.999–1.000)	<.001	1.000 (0.999–1.000)	.009
NLR (ANC/ALC)[a]	1.075 (0.973–1.187)	.156	1.010 (0.906–1.126)	.854
PNI[a]	0.952 (0.925–0.980)	.001	0.944 (0.919–0.969)	<.001
CD3+ T cells[a]	0.996 (0.993–1.000)	.028	0.997 (0.995–1.000)	.074
CD4+ T cells[a]	0.994 (0.990–0.998)	.006	0.995 (0.991–0.999)	.006
CD8+ T cells[a]	0.996 (0.991–1.001)	.138	0.998 (0.993–1.002)	.268
Foxp3+ T cells[a]	0.986 (0.971–1.001)	.062	1.001 (0.990–1.012)	.902
GZB+ T cells[a]	1.003 (0.992–1.014)	.593	1.004 (0.995–1.013)	.414
Foxp3/CD4[a]	1.002 (0.995–1.010)	.539	1.008 (1.002–1.013)	.007
GZB/CD8[a]	1.002 (0.995–1.009)	.668	1.002 (0.996–1.008)	.475
Multivariate analysis[c]				
Sex (Female vs. male)	1.459 (1.012–2.103)	.043		
Stage[b]	3.710 (2.692–5.112)	<.001	2.179 (1.676–2.690)	<.001
ALC[a]	0.999 (0.999–1.000)	.001		
PNI[a]			0.951 (0.925–0.978)	<.001

[a]Continuous variables.
[b]AJCC 7th edition.
[c]Cox regression analysis; forward conditional method was used for the multivariate analysis.
Abbreviations: ALC, absolute lymphocyte count; ANC, absolute neutrophil count; BMI, body mass index; CI, confidence interval; Foxp3, forkhead box P3; GZB, granzyme B; HR, hazard ratio; MSI, microsatellite instability; MSI-H, MSI-high; NLR, neutrophil lymphocyte ratio; PNI, prognostic nutritional index.

associated with RFS (p < .05 for all; Table 2). The multivariate Cox regression analysis using the forward conditional method revealed that sex (p = .043), stage (p < .001), and ALC (p = .001) were independent prognostic factors for poor RFS. Moreover, the univariate analysis for overall survival after surgical resection showed a significant association among tumor size, stage, lymphatic invasion, vascular invasion, neural invasion, ALC, PNI, CD4, and the Foxp3/CD4 ratio and OS (p < .05 for all). The multivariate Cox regression analysis using the forward conditional method revealed that stage (p < .001) and PNI (p < .001) were independent prognostic factors for poor OS.

In the subgroup analysis of patients with MSI-H tumors (Table 3), only stage was significantly associated with RFS and OS. However, in the patients with non-MSI-H tumors, the univariate survival analysis for recurrence after surgical resection showed that age, sex, Lauren classification, tumor size, stage, lymphatic invasion, vascular invasion, neural invasion, ALC, PNI, CD3, and CD4 were significantly associated with RFS (p < .05 for all; Table 3, supplemental online Fig. 3). The multivariate Cox regression analysis using the forward conditional method revealed that age (p = .002), stage (p < .001), PNI (p < .001), and CD4 (p = .040) were independent prognostic factors for poor RFS. The univariate analysis for overall survival after surgical resection showed a significant association between tumor size, disease stage, lymphatic invasion, vascular invasion, neural invasion, ALC, PNI, CD4, and the Foxp3/CD4 ratio and OS (p < .05 for all; Table 3, Fig. 3). The multivariate Cox regression analysis using the forward conditional method revealed that stage (p < .001), PNI (p < .001), and the Foxp3/CD4 ratio (p = .003) were independent prognostic factors for poor OS.

Table 3. Univariate and multivariate Cox regression analyses for overall survival and recurrence-free survival according to clinicopathologic variables and subset of tumor-infiltrating lymphocytes in patients with MSI-H (n = 57) and those with non-MSI-H (n = 288) gastric carcinoma

	Recurrence-free survival		Overall survival	
Variables	**HR (95% CI)**	***p* value**	**HR (95% CI)**	***p* value**
MSI-H group (n = 57)				
Univariate analysis				
Age[a]	0.982 (0.946–1.020)	.359	1.010 (0.977–1.044)	.546
Sex (female vs. male)	0.427 (0.119–1.530)	.191	0.549 (0.199–1.510)	.245
BMI[a]	0.858 (0.720–1.022)	.086	0.952 (0.831–1.090)	.475
Lauren classification (diffuse vs. intestinal, mixed)	2.141 (0.665–6.894)	.202	1.436 (0.514–4.011)	.490
Tumor size[a]	1.012 (0.997–1.027)	.126	1.005 (0.993–1.018)	.403
Stage[b]	3.791 (1.627–8.835)	.002	2.093 (1.124–3.898)	.020
Lymphatic invasion (positive vs. negative)	2.229 (0.460–10.803)	.319	0.743 (0.469–6.477)	.407
Vascular invasion (positive vs. negative)	1.755 (0.511–6.025)	.371	2.318 (0.725–7.406)	.156
Neural invasion (positive vs. negative)	2.449 (0.584–10.267)	.221	2.206 (0.621–7.835)	.221
ANC[a]	1.000 (1.000–1.000)	.487	1.000 (1.000–1.000)	.519
ALC[a]	1.000 (0.999–1.001)	.711	1.000 (1.000–1.001)	.200
NLR (ANC/ALC)[a]	1.180 (0.693–2.011)	.541	1.023 (0.637–1.643)	.925
PNI[a]	1.032 (0.939–1.134)	.518	0.979 (0.910–1.054)	.577
CD3+ T cells[a]	0.999 (0.991–1.007)	.779	0.998 (0.991–1.005)	.578
CD4+ T cells[a]	0.999 (0.989–1.009)	.906	0.999 (0.991–1.007)	.802
CD8+ T cells[a]	1.005 (0.993–1.017)	.429	0.995 (0.984–1.007)	.430
Foxp3+ T cells[a]	1.002 (0.965–1.041)	.991	1.017 (0.986–1.048)	.292
GZB+ T cells[a]	1.005 (0.982–1.028)	.685	1.002 (0.982–1.023)	.822
Foxp3/CD4[a]	1.001 (0.979–1.024)	.913	1.003 (0.986–1.021)	.721
GZB/CD8[a]	1.002 (0.978–1.027)	.850	1.012 (0.995–1.029)	.177
Non-MSI-H group (n = 288)				
Univariate analysis				
Age[a]	0.977 (0.964–0.991)	.001	1.000 (0.987–1.013)	.985
Sex (female vs. male)	1.698 (1.164–2.478)	.006	1.101 (0.774–1.566)	.593
BMI[a]	0.964 (0.906–1.026)	.251	0.950 (0.898–1.006)	.078
Lauren classification (diffuse vs. intestinal, mixed)	1.472 (1.006–2.154)	.047	1.061 (0.742–1.517)	.744
Tumor size[a]	1.012 (1.008–1.015)	<.001	1.011 (1.007–1.015)	<.001
Stage[b]	3.507 (2.533–4.857)	<.001	2.112 (1.663–2.681)	<.001
Lymphatic invasion (positive vs. negative)	3.911 (2.254–6.786)	<.001	2.192 (1.403–3.425)	.001
Vascular invasion (positive vs. negative)	4.068 (2.446–6.766)	<.001	2.461 (1.622–3.733)	<.001
Neural invasion (positive vs. negative)	2.971 (1.835–4.811)	<.001	1.874 (1.228–2.860)	.004
ANC[a]	1.000 (1.000–1.000)	.346	1.000 (1.000–1.000)	.103
ALC[a]	0.999 (0.999–1.000)	<.001	1.000 (0.999–1.000)	.001
NLR (ANC/ALC)[a]	1.067 (0.964–1.182)	.209	1.007 (0.902–1.124)	.903
PNI[a]	0.935 (0.906–0.965)	<.001	0.993 (0.906–0.960)	<.001
CD3+ T cells[a]	0.996 (0.993–1.000)	.038	0.997 (0.994–1.001)	.113
CD4+ T cells[a]	0.993 (0.989–0.998)	.004	0.994 (0.990–0.998)	.004
CD8+ T cells[a]	0.996 (0.990–1.001)	.129	0.999 (0.994–1.004)	.613
Foxp3+ T cells[a]	0.986 (0.970–1.003)	.108	1.000 (0.998–1.012)	.977
GZB+ T cells[a]	1.005 (0.992–1.018)	.451	1.006 (0.995–1.017)	.276
Foxp3/CD4[a]	1.004 (0.997–1.012)	.289	1.009 (1.004–1.015)	.001
GZB/CD8[a]	1.002 (0.994–1.009)	.660	1.001 (0.995–1.007)	.761
Multivariate analysis[c]				
Age[a]	0.977 (0.963–0.991)	.002		
Stage[b]	3.592 (2.519–5.121)	<.001	2.176 (1.681–2.818)	<.001
PNI[a]	0.927 (0.896–0.960)	<.001	0.935 (0.907–0.964)	<.001
CD4+ T cells [a]	0.995 (0.990–1.000)	.040		
Foxp3/CD4[a]			1.013 (1.005–1.022)	.003

[a]Continuous variables.
[b]AJCC 7th edition.
[c]Cox regression analysis; forward conditional method was used for the multivariate analysis.
Abbreviations: ALC, absolute lymphocyte count; ANC, absolute neutrophil count; BMI, body mass index; CI, confidence interval; Foxp3, forkhead box P3; GZB, granzyme; HR, hazard ratio; MSI, microsatellite instability; MSI-H, MSI-high; NLR, neutrophil lymphocyte ratio; PNI, prognostic nutritional index.

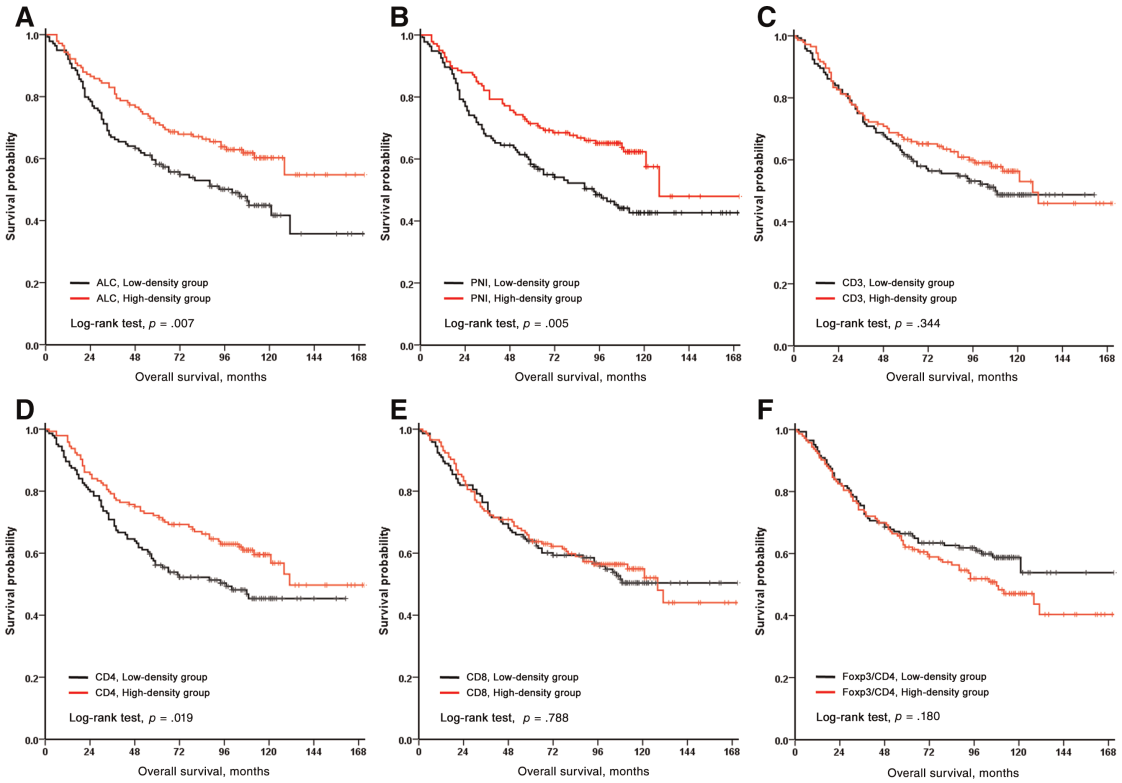

Figure 3. Kaplan-Meier analysis for overall survival according to ALC, PNI, and subsets of tumor-infiltrating lymphocytes in patients with non-MSI-H tumors. Overall survival was plotted against the **(A)** ALC, **(B)** PNI, **(C)** CD3, **(D)** CD4, **(E)** CD8, and **(F)** Foxp3/CD4. Abbreviations: ALC, absolute lymphocyte count; Foxp3, forkhead box P3; PNI, prognostic nutritional index.

The interaction of MSI subgroups for RFS with ALC (hazard ratio [HR], 1.001; 95% confidence interval [CI], 1.000–1.002; p = .009; supplemental online Table 1), PNI (HR, 1.212; 95% CI, 1.082–1.359; p = .001; supplemental online Table 2), CD4 (HR, 1.010; 95% CI, 1.000–1.019; p = .044; supplemental online Table 3), and the Foxp3/CD4 ratio (HR, 0.963; 95% CI, 0.936–0.991; p = .009; supplemental online Table 4) was statistically significant. Also, the interaction of MSI subgroups for OS with ALC (HR, 1.001; 95% CI, 1.001–1.002; p = .001; supplemental online Table 1) and the Foxp3/CD4 ratio (HR, 0.973; 95% CI, 0.951–0.996; p = .021; supplemental online Table 4) was statistically significant.

Discussion

The present study showed that (a) the density of each subset of TILs differed between MSI-H and non-MSI-H tumors; precisely, patients with MSI-H tumors showed significantly increased cytotoxic T cells, activated cytotoxic T cells, and regulatory T cells. (b) The association between systemic/local immune response and prognosis differed according to MSI status. (c) Only a weak association was observed between the systemic and local immune response.

In this study, we evaluated only stromal TILs at tumor center, not invasive margin. According to the recommendation of an international TILs working group, separate reporting of invasive margin and central tumor TILs is recommended in colorectal cancer. The authors recommended that only stromal TILs, not intratumoral TILs, were evaluated in gastric carcinoma. However, there was a lack of evidence for consensus on reporting of invasive margin and central tumor TILs in the upper gastrointestinal tract [32]. As noted, there were several studies for the densities of stromal TILs at the invasive margin in colorectal cancer. The density of each subset of T cells is significantly differed according to location, and lower densities of CD3+ and CD8+ T cells at invasive margin was associated with shorter OS [33, 34]. Unlike in colorectal cancer, the number of poorly cohesive carcinomas is high in stomach cancer. In this study, the number of mixed and diffuse type gastric cancer was 168 (48.7%) cases. The poorly cohesive carcinoma invades with a single tumor cell and does not make the clear invasion margin. Also, there are only a few lymphocytes around singly infiltrative tumor cells. Therefore, only the stromal TILs at central tumor was included in this study.

MSI-H gastric carcinoma is recognized as a major distinct subtype of gastric cancer [35, 36]. Furthermore, the MSI phenotype is known to be strongly associated with immune cell signaling [35]. An intriguing finding of our study was that MSI-H tumors showed a high level of both favorable (CD8+ and granzyme B+ T cells) [37] and unfavorable (Foxp3+ T cells and Foxp3+/CD4+ ratio) [31, 38] prognostic factors at the same time. This paradoxical finding has also been observed in colon cancer, where elevated numbers of cytotoxic T lymphocytes is paralleled by an enhanced infiltration of regulatory T lymphocytes. Taken together, these findings suggest that regulatory T cells may play a role in the regulation of the immune response in MSI-H tumors [9, 39, 40]. Very few studies, and only those regarding colon cancer, have examined the relationship between regulatory T cells and cytotoxic T cells [41]. Yoon et al.

showed that regulatory T cells were prognostic only in cancers with low cytotoxic T cells infiltration [41]. Recently, Llosa et al. showed that there was functional exhaustion and unresponsiveness of T cells that have a concomitant expression of immune checkpoint markers, such as PD-1, PD-L1, LAG-3, and TIM-3 in MSI colorectal cancer [42]. And, the author suggested that the prognosis of colorectal cancer depends on the T lymphocyte exhaustion, and it is the reason MSI tumor are not naturally eliminated despite cancer having a hostile T helper 1 cells (T_H1)/CTL microenvironment. Therefore, the finding of tumor-infiltrating regulatory T cells and cytotoxic T cells should be interpreted within this context. This explains why patients with MSI-H colon and gastric cancers show only a marginal survival benefit despite an abundant infiltration of tumor-infiltrating cytotoxic T cells

In our study, high density of CD4+ T cells was an independent prognostic factor for RFS (p = .040) in patients with non-MSI-H tumors. In a recent meta-analysis of TILs in gastric cancer, CD4+ T cells was not statistically associated with survival [43]. Most of the studies in this meta-analysis did not analyze the group divided by MSI status but analyzed the whole stomach cancer. We also founded that the density of CD4+ T cells was not an independent prognostic factor for OS and RFS in gastric cancer (whole cohort, n = 345).

CD4+ T cells include all subsets of helper T cells and regulatory T cells. T helper cells are divided into several types according to the cytokine produced by the cell. T_H1 cells produce interleukin (IL)-2 and interferon (IFN)γ and act on CD8+ cytotoxic T cells, NK cells, and macrophages. T_H2 cells produce IL-4, IL-5, and IL-13 and act on B cells. T_H17 cells produce IL-17a, IL-21, and IL-22 and are involved in antimicrobial tissue inflammation. In gastric cancer, T_H1 and T_H17 subsets are associated with a good prognosis; however, the T_H2 subset is associated with a poor prognosis [44, 45]. Therefore, future studies should work toward subtyping of helper T cells, which would allow for the determination of whether the density of each subset of helper T cells differs according to MSI status.

Another intriguing finding was that the impact of MSI status increased as cancer progressed. The difference in cytotoxic, regulatory, and activated cytotoxic T lymphocyte infiltration between MSI-H and non-MSI-H tumors was more prominent with tumor progression. Considering that the association between MSI status and TILs was prominent in tumors classified under a high T category, further study on TILs and MSI phenotype in association with tumor progression in gastric cancer are necessary to understand the mechanism of carcinogenesis and the antitumor immune response.

Although the current study represents the largest investigation of the association between the local and systemic immune response according to MSI status, and although this study identified distinguishing characteristics between MSI-H and non-MSI-H tumors using TILs, much remains to be explored. The number of cases of MSI-H tumors included in this study was not large enough to identify a detailed relationship or determine the prognostic value of TILs and MSI status. However, we hope that the findings of our study lay the foundation for designing future studies.

Conclusion

Gastric tumors with microsatellite instability harbor a distinct distribution of TIL subsets, especially in advanced T-classification. The prognostic influence of the systemic and local immune response differs between MSI-H and non-MSI-H tumors. The differing tumor characteristics and prognoses according to MSI status could be associated with the immunogenicity caused by microsatellite instability and subsequent host immune response. The prognostic implications of this relationship may help to identify the mechanisms of cancer progression and develop treatment strategies for MSI-H gastric cancer.

Acknowledgments

This work was supported by the National Research Foundation of Korea grant funded by the Korea government (MSIP; No. 2016R1A2B4014984).

Author Contributions

Conception/design: Su-Jin Shin, Hyoung-Il Kim
Collection and/or assembly of data: Yoon Young Choi, Taeil Son, Jae-Ho Cheong, Woo Jin Hyung, Sung Hoon Noh, Chung-Gyu Park
Data analysis and interpretation: Su-Jin Shin, Sang Yong Kim, Hyoung-Il Kim
Manuscript writing: Su-Jin Shin, Hyoung-Il Kim
Final approval of manuscript: Hyoung-Il Kim

Disclosures

The authors indicated no financial relationships.

References

1. Fridman WH, Pagès F, Sautès-Fridman C et al. The immune contexture in human tumours: Impact on clinical outcome. Nat Rev Cancer 2012;12:298–306.

2. Arigami T, Uenosono Y, Ishigami S et al. Decreased density of CD3+ tumor-infiltrating lymphocytes during gastric cancer progression. J Gastroenterol Hepatol 2014;29:1435–1441.

3. Kang BW, Seo AN, Yoon S et al. Prognostic value of tumor-infiltrating lymphocytes in Epstein-Barr virus-associated gastric cancer. Ann Oncol 2016;27:494–501.

4. Grogg KL, Lohse CM, Pankratz VS et al. Lymphocyte-rich gastric cancer: Associations with Epstein-Barr virus, microsatellite instability, histology, and survival. Mod Pathol 2003;16:641–651.

5. Choi YY, Bae JM, An JY et al. Is microsatellite instability a prognostic marker in gastric cancer? A systematic review with meta-analysis. J Surg Oncol 2014;110:129–135.

6. Fang WL, Chang SC, Lan YT et al. Microsatellite instability is associated with a better prognosis for gastric cancer patients after curative surgery. World J Surg 2012;36:2131–2138.

7. Gajewski TF, Schreiber H, Fu YX. Innate and adaptive immune cells in the tumor microenvironment. Nat Immunol 2013;14:1014–1022.

8. Coulie PG, Van den Eynde BJ, van der Bruggen P et al. Tumour antigens recognized by T lymphocytes: At the core of cancer immunotherapy. Nat Rev Cancer 2014;14:135–146.

9. Michel S, Benner A, Tariverdian M et al. High density of FOXP3-positive T cells infiltrating colorectal cancers with microsatellite instability. Br J Cancer 2008;99:1867–1873.

10. Dahlin AM, Henriksson ML, Van Guelpen B et al. Colorectal cancer prognosis depends on T-cell infiltration and molecular characteristics of the tumor. Mod Pathol 2011;24:671–682.

11. Ottini L, Falchetti M, Lupi R et al. Patterns of genomic instability in gastric cancer: Clinical

implications and perspectives. Ann Oncol 2006; 17(suppl 7):vii97–102.

12. Lee HS, Choi SI, Lee HK et al. Distinct clinical features and outcomes of gastric cancers with microsatellite instability. Mod Pathol 2002;15: 632–640.

13. Seo HM, Chang YS, Joo SH et al. Clinicopathologic characteristics and outcomes of gastric cancers with the MSI-H phenotype. J Surg Oncol 2009;99:143–147.

14. Zhang L, Conejo-Garcia JR, Katsaros D et al. Intratumoral T cells, recurrence, and survival in epithelial ovarian cancer. N Engl J Med 2003; 348:203–213.

15. Perrone G, Ruffini PA, Catalano V et al. Intratumoural FOXP3-positive regulatory T cells are associated with adverse prognosis in radically resected gastric cancer. Eur J Cancer 2008; 44:1875–1882.

16. Wang B, Xu D, Yu X et al. Association of intra-tumoral infiltrating macrophages and regulatory T cells is an independent prognostic factor in gastric cancer after radical resection. Ann Surg Oncol 2011

17. Lee HE, Chae SW, Lee YJ et al. Prognostic implications of type and density of tumour-infiltrating lymphocytes in gastric cancer. Br J Cancer 2008;99:1704–1711.

18. Chiaravalli AM, Feltri M, Bertolini V et al. Intratumour T cells, their activation status and survival in gastric carcinomas characterised for microsatellite instability and Epstein-Barr virus infection. Virchows Arch 2006;448:344–353.

19. Mori K, Toiyama Y, Saigusa S et al. Systemic analysis of predictive biomarkers for recurrence in colorectal cancer patients treated with curative surgery. Dig Dis Sci 2015;60:2477–2487.

20. Roxburgh CS, McMillan DC. Role of systemic inflammatory response in predicting survival in patients with primary operable cancer. Future Oncol 2010;6:149–163.

21. Porrata LF, Ristow K, Habermann TM et al. Absolute lymphocyte count at the time of first relapse predicts survival in patients with diffuse large B-cell lymphoma. Am J Hematol 2009;84: 93–97.

22. Dutta S, Going JJ, Crumley AB et al. The relationship between tumour necrosis, tumour proliferation, local and systemic inflammation, microvessel density and survival in patients undergoing potentially curative resection of oesophageal adenocarcinoma. Br J Cancer 2012;106:702–710.

23. Park JH, Powell AG, Roxburgh CS et al. Mismatch repair status in patients with primary operable colorectal cancer: Associations with the local and systemic tumour environment. Br J Cancer 2016;114:562–570.

24. Wang J, Wang S, Song X et al. The prognostic value of systemic and local inflammation in patients with laryngeal squamous cell carcinoma. Onco Targets Ther 2016;9:7177–7185.

25. Turner N, Wong HL, Templeton A et al. Analysis of local chronic inflammatory cell infiltrate combined with systemic inflammation improves prognostication in stage II colon cancer independent of standard clinicopathologic criteria. Int J Cancer 2016;138:671–678.

26. Choi Y, Kim JW, Nam KH et al. Systemic inflammation is associated with the density of immune cells in the tumor microenvironment of gastric cancer. Gastric Cancer 2017;20:602–611.

27. American Joint Committee on Cancer. AJCC Cancer Staging Manual. New York, NY: Springer, 2010:648

28. Lee JY, Kim HI, Kim YN et al. Clinical significance of the prognostic nutritional index for predicting short- and long-term surgical outcomes after gastrectomy: A retrospective analysis of 7781 gastric cancer patients. Medicine (Baltimore) 2016; 95:e3539.

29. Kim H, An JY, Noh SH et al. High microsatellite instability predicts good prognosis in intestinal-type gastric cancers. J Gastroenterol Hepatol 2011; 26:585–592.

30. Boland CR, Thibodeau SN, Hamilton SR et al. A national cancer institute workshop on microsatellite instability for cancer detection and familial predisposition: Development of international criteria for the determination of microsatellite instability in colorectal cancer. Cancer Res 1998;58: 5248–5257.

31. Kim HI, Kim H, Cho HW et al. The ratio of intra-tumoral regulatory T cells (Foxp3+)/helper T cells (CD4+) is a prognostic factor and associated with recurrence pattern in gastric cardia cancer. J Surg Oncol 2011;104:728–733.

32. Hendry S, Salgado R, Gevaert T et al. Assessing tumor-infiltrating lymphocytes in solid tumors: A practical review for pathologists and proposal for a standardized method from the international immuno-oncology biomarkers working group: Part 2: TILs in melanoma, gastrointestinal tract carcinomas, non-small cell lung carcinoma and mesothelioma, endometrial and ovarian carcinomas, squamous cell carcinoma of the head and neck, genitourinary carcinomas, and primary brain tumors. Adv Anat Pathol 2017;24:311–335.

33. Yoon HH, Shi Q, Heying EN et al. Intertumoral heterogeneity of CD3(+) and CD8(+) T-cell densities in the microenvironment of DNA mismatch-repair-deficient colon cancers: Implications for prognosis. Clin Cancer Res 2019;25:125–133.

34. Pagès F, Mlecnik B, Marliot F et al. International validation of the consensus immunoscore for the classification of colon cancer: A prognostic and accuracy study. Lancet 2018;391:2128–2139.

35. Cancer Genome Atlas Research Network. Comprehensive molecular characterization of gastric adenocarcinoma. Nature 2014;513:202–209.

36. Cristescu R, Lee J, Nebozhyn M et al. Molecular analysis of gastric cancer identifies subtypes associated with distinct clinical outcomes. Nat Med 2015;21:449–456.

37. Shankaran V, Ikeda H, Bruce AT et al. IFNgamma and lymphocytes prevent primary tumour development and shape tumour immunogenicity. Nature 2001;410:1107–1111.

38. Huang Y, Wang FM, Wang T et al. Tumor-infiltrating FoxP3+ Tregs and CD8+ T cells affect the prognosis of hepatocellular carcinoma patients. Digestion 2012;86:329–337.

39. Le Gouvello S, Bastuji-Garin S, Aloulou N et al. High prevalence of Foxp3 and IL17 in MMR-proficient colorectal carcinomas. Gut 2008;57:772–779.

40. Houston AM, Michael-Robinson JM, Walsh MD et al. The "fas counterattack" is not an active mode of tumor immune evasion in colorectal cancer with high-level microsatellite instability. Human Pathol 2008;39:243–250.

41. Yoon HH, Orrock JM, Foster NR et al. Prognostic impact of FoxP3+ regulatory T cells in relation to CD8+ T lymphocyte density in human colon carcinomas. PloS One 2012;7:e42274.

42. Llosa NJ, Cruise M, Tam A et al. The vigorous immune microenvironment of microsatellite instable colon cancer is balanced by multiple counter-inhibitory checkpoints. Cancer Discov 2015;5:43–51.

43. Zheng X, Song X, Shao Y et al. Prognostic role of tumor-infiltrating lymphocytes in gastric cancer: A meta-analysis. Oncotarget 2017;8:57386–57398.

44. Ubukata H, Motohashi G, Tabuchi T et al. Evaluations of interferon-gamma/interleukin-4 ratio and neutrophil/lymphocyte ratio as prognostic indicators in gastric cancer patients. J Surg Oncol 2010; 102:742–747.

45. Chen JG, Xia JC, Liang XT et al. Intratumoral expression of IL-17 and its prognostic role in gastric adenocarcinoma patients. Int J Biol Sci 2011;7:53–60.

See http://www.TheOncologist.com for supplemental material available online.